Bose-stimulated pion production in relativistic nuclear collisions

I.N. Mishustin,[1,2] L.M. Satarov,[1] J.A. Maruhn,[3] H. Stöcker,[3] and W. Greiner[3]
[1] *The Kurchatov Institute, Russian Scientific Center, Moscow 123182, Russia*
[2] *The Niels Bohr Institute, University of Copenhagen, Blegdamsvej 17, DK-2100 Copenhagen Ø, Denmark*
[3] *Institut für Theoretische Physik, J.W. Goethe Universität, D-60054 Frankfurt am Main, Germany*
(Received 28 July 1994)

We demonstrate the importance of the Bose-statistical effects for pion production in relativistic heavy-ion collisions. The evolution of the pion phase-space density in central collisions of ultrarelativistic nuclei is studied in a simple kinetic model taking into account the effect of Bose-stimulated pion production by the NN collisions in a dense cloud of mesons. It is assumed that pions are produced within a finite formation time at the stage of the projectile-target interpenetration. The mutual slowing down of nuclei is described schematically by introducing an effective deceleration length. The role of the quasideuteron and Δ-isobar mechanisms of pion absorption is investigated. The model predicts the enhancement of the soft pion yield as compared to inclusive pp data. The effect is sensitive to the pion formation time and is more pronounced at midrapidity and for heavy nuclei. The results are compared with pion spectra observed in central 10.7A GeV Au+Au and 200A GeV S+S collisions. We suggest new experiments sensitive to the Bose enhancement phenomena.

PACS number(s): 25.75.+r

I. INTRODUCTION

It was observed in CERN experiments [1, 2] that the low p_T component of pion spectra in central heavy-ion collisions at 200 GeV/nucleon is enhanced as compared with the normalized $pp \to \pi X$ data. The analogous enhancement was discovered earlier in high-multiplicity pp [3] and $\alpha\alpha$ [4] collisions. This "soft pion puzzle" has attracted much attention in recent years (see, e.g., [5–11]). Many authors try to explain the effect by the resonance decays and pion rescatterings starting from some (nonenhanced) phase-space distributions of these particles in the initial state [8–10]. In Refs. [12, 13] we proposed a new mechanism which may be responsible, at least partly, for the enhanced yield of soft pions. This effect is explained by the increased (Bose-stimulated) rate of inelastic processes $NN \to \pi$ inside a dense pion cloud produced at earlier stages of the nuclear collision.

The model-independent estimates [12] based on the observed pion spectra in central S+S collisions at 200A GeV show large values of the pion phase-space occupation number, $n_\pi \sim 5$, at small p_T in the central rapidity region [14]. Soft pion occupation numbers of the same order of magnitude were obtained in Ref. [15]. By the analogy to the Bose-stimulated emission of photons in atomic processes, the probability of producing a new pion in an elementary collision of hadrons [16] may be enhanced as compared with the vacuum value if other pions are present nearby in the phase space. The enhancement factor, $n_\pi + 1$, can be significant if $n_\pi \gtrsim 1$.

To estimate qualitatively the observable effects of this Bose-stimulated pion emission we developed a simple model [12, 13] based on the exact solution of the kinetic equation for the pion phase-space distribution function. As in the convolution model it is assumed that pions are produced in binary collisions of nucleons at the stage of the projectile-target interpenetration. A finite formation time of pions [17, 18] is taken into account by assuming that a pion goes on the mass shell (is hadronized) with some delay after the corresponding NN interaction. As shown in [12, 13], the effects of Bose-stimulated pion production can be noticeable only if the duration of the projectile-target interaction exceeds the pion formation time, i.e., for heavy combinations of nuclei [19].

In Refs. [12, 13] few simplifying assumptions were introduced. In particular, the slowing down and excitation of the colliding nuclei were disregarded (free-streaming approximation). Neglecting the energy losses of interacting nucleons results in an overestimation of pion multiplicities by a factor ~ 2 in the case of medium and heavy nuclei at CERN energies. The multifluid model has been developed in Refs. [20, 21], where the finite stopping power of the nuclei is taken into account. This model reproduces the pion multiplicity observed in central 200 GeV/nucleon S+S collisions. On the other hand, in Refs. [20, 21] the effects of the Bose-enhanced pion production have not been included.

Here a more realistic version of the model is presented which takes into account the projectile-target deceleration as well as pion absorption effects. A more detailed analysis of possible signatures of the Bose-stimulated pion emission is performed. The main goal of this work is to find observables most sensitive to the Bose-enhancement (BE) effects.

The paper is organized as follows: Section II is devoted to the description of the model. A generalized kinetic equation for the pion phase-space occupation number is introduced. The gain and loss terms are evaluated and the basic approximations of the model are discussed. In Sec. III the solution of the kinetic equation is investigated. First we consider the BE effects in absence of the projectile-target deceleration and pion absorption. Then

the general case is studied both qualitatively and numerically. The model predictions for pion spectra in central 200A GeV S+S and 10.7A GeV Au+Au collisions are compared with the existing experimental data. Some recommendations for future experimental studies are given. Section IV is reserved for concluding remarks and discussion.

II. DESCRIPTION OF THE MODEL

In this section we present the simple kinetic model of pion production in relativistic nuclear collisions. It is a natural extension of the convolution model, but takes into account deceleration of the colliding nucleons, pion absorption, and the effects of Bose-stimulated pion emission.

A. The kinetic equation for pion phase-space distribution

As already stated, we consider the hadronic scenario of nuclear collisions. Only the pion and nucleon degrees of freedom are included explicitly. Possible modifications due to the formation and decay of meson and baryon resonances will be discussed later. The coupled kinetic equations describing the dynamics of pions and nucleons in high-energy heavy-ion collisions have been proposed in Refs. [22, 23]. The two-particle collision integrals entering these equations were expressed via the inclusive cross sections of the elementary processes $a+b \to c+X$, where $a, b, c = N, \pi$. The numerical realizations of this model within the multifluid approximation were described in Refs. [20, 24]. In the present paper this kinetic approach is generalized by taking into account the pion formation time, pion absorption in πNN interactions and the Bose-stimulated pion emission.

To simplify the problem, in the present version of the model we do not treat the space-time evolution of nucleons self-consistently, but use a parametrization of their phase-space distribution functions (see Sec. II C). Another important approximation (which makes the model more tractable) is the neglect of $\pi\pi$ rescatterings for pions produced in different NN collisions. As discussed in Refs. [8, 25], at $\sqrt{s_{\pi\pi}} \lesssim 0.7$ GeV, the $\pi\pi$ interactions are mostly elastic, i.e., do not change the number of pions, but only change their distribution in the phase space. It was shown in Ref. [10] that the total $\pi\pi$ cross section in a dense cloud of secondary pions may be considerably reduced as compared with the vacuum value. On the other hand, the in-medium $\pi\pi$ cross section contains the enhancement factor $n_\pi + 1$ which leads to the preferential scattering of pions to the phase-space regions with high n_π. According to Refs. [8, 10] this may increase the pion yield at low p_T.

Let us denote by $n_\pi(x, \vec{p})$ the dimensionless single-particle distribution function (occupation number) of pions with momentum $\vec{p}$ in a given space-time point $x = (t, \vec{r})$. In the quasiclassical approximation and disregarding possible isospin effects, one can consider the quantity

$$f_\pi(t, \vec{r}, \vec{p}) = \frac{g_\pi}{(2\pi\hbar)^3} n_\pi(x, \vec{p}) \equiv \frac{1}{\zeta} n_\pi(x, \vec{p}) \tag{1}$$

as the phase-space density of pions in a point with coordinates $(\vec{r}, \vec{p})$ at time t. In the above expression $g_\pi = 3$ is the spin-isospin degeneracy factor for pions, and $\zeta = (2\pi\hbar)^3/3$ is introduced for brevity.

We proceed from the following relativistic kinetic equation for n_π (units $c = 1$ are used throughout the paper):

$$p^i \frac{\partial}{\partial x^i} n_\pi(x, \vec{p}) = G(x, \vec{p}) - \Lambda_a(x, \vec{p})\, n_\pi(x, \vec{p}), \tag{2}$$

where $p^i = (E_\pi, \vec{p})^i$ is the pion four-momentum, $E_\pi = \sqrt{m_\pi^2 + \vec{p}^{\,2}}$ and m_π is the pion mass. The gain (source) term $G(x, \vec{p})$ describes the rate of pion production in the inelastic NN collisions. The last term on the right-hand side of Eq. (2) corresponds to the local rate of pion absorption [26]. The absorption coefficient Λ_a will be derived in Sec. II B.

Let us consider first the limit of zero pion formation time and disregard the BE effects. In this case the gain term has the form [22, 23]

$$G_0(x, \vec{p}) = \frac{\zeta}{2} \int d^3 p_1 f_N(x, \vec{p}_1) \int d^3 p_2 f_N(x, \vec{p}_2) \sqrt{(\vec{v}_1 - \vec{v}_2)^2 - (\vec{v}_1 \times \vec{v}_2)^2}\, \sigma_{\rm inv}(\sqrt{s}, \vec{p}). \tag{3}$$

Here $f_N(x, \vec{p})$ is the phase-space distribution function of nucleons, normalized to the baryon density (after integrating over the momentum space), and $\vec{v}_{1,2}$ are nucleon velocities. The last factor in Eq. (3)

$$\sigma_{\rm inv}(\sqrt{s}, \vec{p}) = E_\pi \frac{d\sigma_{NN \to \pi X}}{d^3 p} \tag{4}$$

is the invariant differential cross section of the inclusive reaction $NN \to \pi X$, summed over all charge states of a secondary pion and averaged over the isospin components of colliding nucleons. It is a function of $\vec{p}$ and the total c.m. energy (squared) of a nucleon pair, $s = (p_1 + p_2)^2$. In our calculations we use the parametrization of the $NN \to \pi X$ cross section described in Ref. [13].

Following Refs. [12, 13] we incorporate the effects of the Bose-stimulated pion production by inserting an additional factor $n_\pi + 1$ into the gain term of the kinetic equation [27]. The delayed character of pion emission is taken into account in the same way as in Ref. [28], by the replacement $x \to x' = (t - \tau_f, \vec{r} - \vec{v}\tau_f)$ in the source term of Eq. (2). Here $\vec{v} = \vec{p}/E_\pi$ is the pion velocity and $\tau_f = \tau_f(\vec{p})$ is the formation time of pion with the momentum $\vec{p}$ in a single NN collision. $\tau_f(\vec{p})$ is parametrized as follows [28]:

$$\tau_f = \tau_0 \cdot \frac{E_\pi}{m_\pi} = \frac{\tau_0}{\sqrt{1-\vec{v}^2}}, \tag{5}$$

where $\tau_0 \gtrsim \hbar/m_\pi \sim 1$ fm/c is the formation time in the pion rest frame [29]. The modified gain term can be written as

$$G(x,\vec{p}) = G_0(x',\vec{p}) \cdot [1 + n_\pi(x',\vec{p})], \tag{6}$$

where $G_0(x,\vec{p})$ is given by Eq. (3) and

$$x' = x - \tau_0 \frac{p}{m_\pi}. \tag{7}$$

Due to the shift in the argument of the gain term, the resulting kinetic equation is nonlocal in space-time coordinates.

At ultrarelativistic energies the colliding nuclei are partially transparent, at least at the initial stage of the nuclear collision [24]. Following Ref. [30] we describe the nuclear collision as an interaction of two interpenetrating baryonic flows originating from the projectile and target nucleons. As in the two-fluid model we parametrize the nucleon distribution function $f_N(x,\vec{p})$ by the sum of two components separated in the momentum space and corresponding to the projectile ($\alpha = p$) and target ($\alpha = t$) flows. Disregarding the spread of the momentum distribution of nucleons inside each flow, we write [23, 24]

$$f_N(x,\vec{p}) = \sum_{\alpha=p,t} \rho_\alpha U_\alpha^0 \, \delta(\vec{p} - m_N \vec{U}_\alpha), \tag{8}$$

where m_N is the nucleon mass, $\rho_\alpha = \rho_\alpha(x)$ and $U_\alpha^i = U_\alpha^i(x) = (U_\alpha^0, \vec{U}_\alpha)^i$ are, respectively, the rest-frame baryon density and four-velocity of the α flow in a space-time point x.

Substituting (8) into Eq. (3) and taking into account only the contribution of (more violent) interflow NN collisions [31] we get

$$G_0(x,\vec{p}) = \zeta \, \nu_{NN}(x) \, \sigma_{\rm inv}(\sqrt{s_0},\vec{p}). \tag{9}$$

Here $s_0 = m_N^2 \cdot (U_p + U_t)^2$ and the quantity

$$\nu_{NN}(x) = \rho_p \rho_t \sqrt{(U_p U_t)^2 - 1} \tag{10}$$

is proportional to the local rate of the NN collisions. The latter is nonzero at the stage of the nuclear geometrical overlap, when $\rho_p \rho_t \neq 0$. The source is fully determined if the space-time evolution of ρ_α and U_α^i is known.

It is convenient to represent the kinetic equation for the pion occupation number in a noncovariant form, dividing it by E_π. Using Eqs. (2), (6), (9) we obtain

$$\left(\frac{\partial}{\partial t} + \vec{v}\frac{\partial}{\partial \vec{r}}\right) n_\pi(x,\vec{p}) = \lambda(x',\vec{p})\,[1 + n_\pi(x',\vec{p})] - \lambda_a(x,\vec{p}) n_\pi(x,\vec{p}), \tag{11}$$

where

$$\lambda(x,\vec{p}) \equiv G_0(x,\vec{p})/E_\pi = \zeta \, \nu_{NN}(x) \left.\frac{d\sigma_{NN\to\pi X}}{d^3p}\right|_{s=s_0} \tag{12}$$

and

$$\lambda_a(x,\vec{p}) \equiv \Lambda_a(x,\vec{p})/E_\pi \tag{13}$$

are, respectively, the pion production and absorption rates at given x and $\vec{p}$.

The transition to new spatial variables, $\vec{r} \to \vec{r} + \vec{v}\,t$, yields the transformed functions marked by tildes:

$$\left\{\begin{array}{c}\tilde{n}_\pi \\ \tilde{\lambda} \\ \tilde{\lambda}_a\end{array}\right\}(t,\vec{r},\vec{p}) \equiv \left\{\begin{array}{c} n_\pi \\ \lambda \\ \lambda_a\end{array}\right\}(t,\vec{r}+\vec{v}\,t,\vec{p}). \tag{14}$$

This change of variables is equivalent to the transition into the pion rest frame, where the interacting nuclei acquire an additional velocity $-\vec{v}$. By using Eq. (14) one can rewrite the kinetic equation (11) in the form where $\vec{r}$ and $\vec{p}$ enter only as parameters:

$$\dot{\tilde{n}}_\pi(t) = \tilde{\lambda}(t-\tau_f) \cdot [1 + \tilde{n}_\pi(t-\tau_f)] - \tilde{\lambda}_a(t)\,\tilde{n}_\pi(t). \tag{15}$$

Here the arguments $\vec{r},\vec{p}$ are omitted for brevity and $\dot{\tilde{n}}_\pi(t) \equiv \frac{\partial}{\partial t}\tilde{n}_\pi(t,\vec{r},\vec{p})$.

Equation (15) is an ordinary differential equation which can be formally solved by iterations for arbitrary $\tilde{\lambda}(t)$ and $\tilde{\lambda}_a(t)$. Using the boundary condition $\tilde{n}_\pi(-\infty) = 0$ one can represent this equation in the integral form

$$\tilde{n}_\pi(t) = \int_{-\infty}^{t-\tau_f} dt_1 \Phi(t,t_1) \cdot [1 + \tilde{n}_\pi(t_1)], \tag{16}$$

where

$$\Phi(t,t_1) \equiv \tilde{\lambda}(t_1) \cdot \exp\left(-\int_{t_1+\tau_f}^{t} d\tau \tilde{\lambda}_a(\tau)\right). \tag{17}$$

Note that the pion absorption exponent contains explicitly the pion formation time. One can see that absorption effects become weaker with raising τ_f. In particular, this takes place at high c.m. pion momenta due to the strong energy dependence of τ_f [see Eq. (5)].

Below we assume sharp boundaries of interacting nuclei (see Sec. II C). In this approximation $\tilde{\lambda}(t)$ is nonzero within the time interval $t_- < t < t_+$ where $t_\pm = t_\pm(\vec{r},\vec{p})$ are the minimal (t_-) and maximal (t_+) times for the pion production in the phase-space point $(\vec{r},\vec{p})$. They correspond to the roots of the pion production rate [32]:

$$\tilde{\lambda}(t_\pm) = 0. \tag{18}$$

The second term in square brackets of Eq. (16) gives the contribution of the BE effects. Omitting this contribution, we get the lowest-order approximation to $\tilde{n}_\pi(t)$:

$$n_0(t) = \int_{t_-}^{t-\tau_f} dt_1 \Phi(t,t_1). \tag{19}$$

It is nonzero at $t > t_- + \tau_f$. In a general case the solution of Eq. (16) can be represented as a sum over iterations

$$\tilde{n}_\pi(t) = \sum_{k=0}^{k_{\max}} \Theta\,[t - t_- - (k+1)\tau_f]\; n_k(t), \tag{20}$$

$$n_k(t) = \int_{t_- + k\tau_f}^{t-\tau_f} dt_1 \Phi(t,t_1)\, n_{k-1}(t_1)\ , \tag{21}$$

where $\Theta(x) \equiv (1+\mathrm{sgn}\, x)/2$ and $k_{\max} = [(t_+ - t_-)/\tau_f]$. The terms $n_k(t)$ with $k \geq 1$ in Eq. (20) are responsible for the Bose-stimulated emission of pions. They are nonzero if $k_{\max} \geq 1$. Therefore, the Bose-enhanced pion production in a given phase-space point is possible only under condition

$$t_+ - t_- > \tau_f\ . \tag{22}$$

This condition will be further discussed in Sec. II D.

The asymptotic behavior of the pion phase-space distribution at $t \to \infty$ determines the observable pion spectra. For pions of a given charge, e.g., π^-, we have

$$\frac{dN_{\pi^-}}{d^3p} = (2\pi\hbar)^{-3} \lim_{t\to\infty} \int d^3r\, n_\pi(x,\vec{p}) = (2\pi\hbar)^{-3} \lim_{t\to\infty} \int d^3r\, \tilde{n}_\pi(t)\ . \tag{23}$$

Due to the neglect of isospin effects, the same spectra are predicted also for π^0 and π^+ mesons. The pion distribution in the longitudinal rapidity $y \equiv \mathrm{arctanh}(v_\parallel)$ can be obtained from Eq. (23) by multiplying it by $E_\pi = \sqrt{m_\pi^2 + \vec{p}_T^{\,2}}\cosh y$ and integrating over the transverse momentum $\vec{p}_T$.

B. Pion absorption cross section

In this section we discuss the parametrization of the absorption coefficient $\Lambda_a(x,\vec{p})$ introduced in Eq. (2). It is well known that the pion absorption on a free single nucleon is forbidden and at least two nucleons should participate in this process. The quantity Λ_a is represented as a sum of two components describing absorption of pions in the projectile and target nuclei:

$$\Lambda_a = \sum_{\alpha=p,t} \Lambda_{a\alpha}\ , \tag{24}$$

where $\Lambda_{a\alpha}$ corresponds to the rate of pion absorption in the α flow. We do not include pion absorption on a pair of nucleons from different flows because this process should be suppressed by the high Lorentz factor of their relative motion.

Let us make transition to the local rest frame of the α flow denoting the corresponding quantities by primes. Then the pion energy may be written as

$$E'_\alpha = \sqrt{m_\pi^2 + |\vec{p}\,'_\alpha|^2} = (pU_\alpha)\,, \tag{25}$$

where $\vec{p}\,'_\alpha$ is the pion three-momentum. The quantity $\Lambda_{a\alpha}/E'_\alpha$ is the inverse absorption time for a pion in the α-flow rest frame [see Eq. (2)]. Assuming the two-nucleon mechanism of pion absorption one can write $\Lambda_{a\alpha} \propto \rho_\alpha^2 \sigma_{\rm abs}(E'_\alpha)$, where $\sigma_{\rm abs}$ is the effective cross section in nuclear matter at normal density $\rho_0 = 0.17\ \mathrm{fm}^{-3}$. As a result, we obtain the relation [33]

$$\frac{\Lambda_{a\alpha}}{E'_\alpha} = \frac{\rho_\alpha^2}{\rho_0} v'_\alpha \sigma_{\rm abs}(E'_\alpha)\,, \tag{26}$$

where v'_α is the pion velocity relative to the α flow. Substituting Eq. (26) into Eq. (24) we get

$$\Lambda_a = E_\pi \lambda_a = \sum_{\alpha=p,t} \frac{\rho_\alpha^2}{\rho_0} |\vec{p}\,'_\alpha| \sigma_{\rm abs}(E'_\alpha)\,. \tag{27}$$

Here we consider two mechanisms of pion absorption. The first one is the direct (quasideuteron) absorption of a pion by the correlated pn pair with the total isospin I=0. The experimental data show [33, 34] that the NN pairs with I=1 give a relatively small contribution. The most effective absorption takes place for internucleon distances $\lesssim \frac{\hbar}{\sqrt{m_\pi m_N}} \simeq 0.55$ fm. As compared to a free deuteron, the probability to find such a short-range pn correlation in normal nuclear matter is higher by factor of about 3 [35]. On the other hand, the pn pairs with I=0 have the relative weight 1/4. Both factors roughly compensate each other. Therefore for the quasideuteron component of $\sigma_{\rm abs}$ we use the vacuum $\pi^+ d \to pp$ cross section for which analytic parametrization is suggested in Ref. [36]. The energy dependence of $\sigma_{\pi^+ d\to pp}$ is displayed in Fig. 1. Note that the $1/v'$ behavior of this cross section at small v' does not lead to very large values of the absorption rate because of the compensating factor v' [see Eq. (26)].

In addition to the quasideuteron mechanism we take into account the pion absorption via the intermediate formation of the Δ isobar. It is a two-step, essentially nonlocal process: first a pion is captured in a Δ isobar ($\pi N \to \Delta$) which is later absorbed in a collision with another nucleon ($\Delta N \to NN$). We describe this component of pion absorption by the $\pi N \to \Delta$ cross section multiplied by the probability W_Δ to absorb Δ in subsequent ΔN interactions. Therefore, we use the following approximate expression for the pion absorption cross section:

$$\sigma_{\rm abs}(E) = \sigma_{\pi d\to pp}(E) + W_\Delta \sigma_{\pi N\to\Delta}(E)\,, \tag{28}$$

where W_Δ is treated as an energy-independent constant.

To evaluate W_Δ rigorously, one should introduce explicitly the Δ degrees of freedom and determine their phase-space distribution. In principle this can be done by

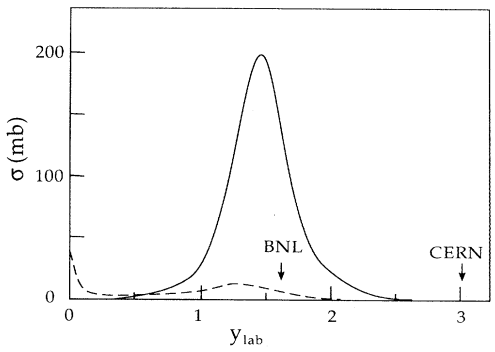

FIG. 1. The $\pi d \to pp$ (dashed line) and $\pi N \to \Delta$ (solid line) cross sections vs pion rapidity in the laboratory frame. Arrows show the initial rapidities of pions produced at zero c.m. momentum at the bombarding energies 200 (CERN) and 10.7 (BNL) GeV/nucleon.

solving the coupled-channel kinetic equations for Δ, N, and π particles. To simplify the problem we estimate only the average value of W_Δ which is a function of the ratio λ_Δ/R, where λ_Δ is the Δ mean free path in nuclear matter and R is the characteristic size of the projectile or target nucleus (below we consider only central collisions of identical nuclei). We assume that Δ isobars are produced with an isotropic momentum distribution at random positions inside a spherical domain of nuclear matter of radius R. Then W_Δ is calculated as the volume averaged absorption probability of a Δ particle. Taking $\lambda_\Delta \simeq \lambda_N \simeq 2$ fm at normal nuclear density, we estimated W_Δ for typical medium and heavy nuclei. The resulting values used in the calculations are

$$W_\Delta = \begin{cases} 0.5 \text{ for S+S,} \\ 1 \quad \text{for Au+Au.} \end{cases} \tag{29}$$

As one can see from Fig. 1, the $\pi N \to \Delta$ cross section is much higher than $\sigma_{\pi d \to pp}$ at pion kinetic energies $T_\pi \gtrsim 100$ MeV (we use the parametrization of $\sigma_{\pi N \to \Delta}$ given in Ref. [37]). However, this does not imply that one may disregard the contribution of the quasideuteron mechanism. As we will see below, the latter may be rather important for the absorption of soft (in the c.m. frame) pions at late stages of nuclear collisions. Indeed, due to the projectile-target mutual slowing down the energy of soft pions may be well below the Δ-absorption peak even at high bombarding energies. In addition, more time is available for the absorption of soft pions at low pion-nucleon relative velocities.

C. Space-time picture of a nuclear collision

The main problem in solving the kinetic equation (2) is associated with the space-time evolution of the densities and four-velocities of baryonic flows which determine the pion production and absorption rates, λ and λ_a (see Sec. II A). In this work we use a rather crude approximation of the dynamics of baryonic matter in a heavy-ion collision. Therefore, the numerical results should be taken with caution. On the other hand, we think that the model is quite reasonable, at least on the qualitative level.

As in Refs. [20, 38], we assume that at the stage of the projectile-target interpenetration both nuclei move as "rigid bodies" along the beam axis and describe them as Lorentz-contracted ellipsoids of homogeneous rest-frame density $\rho_{p,t} = \rho_0$. Therefore, the spatial variations of density and four-velocity are neglected within each baryonic flow as well as compression [39] and transverse motion of the projectile and target matter. Below the z axis is chosen along the beam direction and ξ_α denotes the longitudinal coordinates of the projectile ($\alpha = p$) and target ($\alpha = t$) center at a given time t. The calculations are performed in the equal velocity (e.v.) frame where colliding nuclei move with the velocities

$$\dot{\xi}_p = -\dot{\xi}_t \equiv \dot{\xi} \tag{30}$$

and have the Lorentz factor $\gamma = (1 - \dot{\xi}^2)^{-1/2}$ (see Fig. 2). In the case of a central collision of identical nuclei their four-velocities can be written as

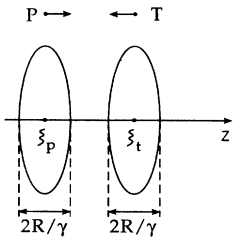

FIG. 2. Geometrical picture of a central collision of equal nuclei in the e.v. frame.

$$U^i_\alpha = (\gamma,\, 0,\, 0,\, \pm\gamma\dot{\xi})^i \,. \tag{31}$$

The rest-frame densities of the baryonic flows can be expressed as follows:

$$\rho_\alpha = \rho_0\, \Theta\left\{R^2 - \vec{r}_\perp^{\,2} - \gamma^2(t)\,[z \mp \xi(t)]^2\right\} \,. \tag{32}$$

Here the upper (lower) sign corresponds to the projectile (target) nucleus, R is the radius of initial nuclei, $\vec{r}_\perp = (x, y)$ are spatial coordinates in the transverse plane.

In the general case, the values of $\dot{\xi}, \gamma$ decrease with time due to the mutual deceleration of the interacting nuclei. Choosing $t = 0$, $\vec{r} = 0$ as a point of the first contact, one can write the initial conditions, determining the trajectory of the projectile $\xi(t) \equiv \xi_p(t)$ as

$$\xi(0) = -R/\gamma_0 \,, \tag{33}$$

$$\dot{\xi}(0) = v_0 \,, \tag{34}$$

where v_0 is the initial c.m. velocity of the nucleons and $\gamma_0 \equiv (1 - v_0^2)^{-1/2}$. The initial Lorentz factor is related to the bombarding energy per nucleon in the laboratory frame $E_{\rm lab}$:

$$\gamma_0 = (1 + E_{\rm lab}/2m_N)^{1/2} \,. \tag{35}$$

The procedure of calculating $\xi(t)$ will be described in the next section. The trajectory of the target center can be found from the symmetry relation: $\xi_t(t) = -\xi(t)$.

Inserting Eqs. (31) and (32) into Eqs. (12) and (10), we obtain

$$\tilde{\lambda}(t) = \lambda_0(t) \cdot \Theta(t_+ - t)\Theta(t - t_-) \,, \tag{36}$$

where tilded quantities are defined in Eq. (14) and

$$\lambda_0(t) = 2\zeta\,(\rho_0\gamma)^2\,\dot{\xi}\,\left.\frac{d\sigma_{NN\to\pi X}}{d^3p}\right|_{\sqrt{s}=2m_N\gamma} \,. \tag{37}$$

In Eq. (36) we assume that $\tilde{\lambda} \neq 0$ in the time interval (t_-, t_+) [see Eq. (18)]. According to Eqs. (12) and (14), the latter condition is equivalent to $\tilde{\nu}_{NN}(t) \cdot \sigma_{\rm inv}(2m_N\gamma, \vec{p}) \neq 0$. By using Eqs. (10) and (32), it can be shown that the corresponding time interval exists only if the conditions

$$(\vec{r}_\perp + \vec{v}_T\, t)^2 + \gamma(t)^2 \cdot [z + v_\parallel\, t - \xi(t)]^2 < R^2 \,, \tag{38}$$

$$(\vec{r}_\perp + \vec{v}_T\, t)^2 + \gamma(t)^2 \cdot [z + v_\parallel\, t + \xi(t)]^2 < R^2 \ , \tag{39}$$

$$\gamma(t) > \gamma_{\rm thr} \equiv [E_\pi + \sqrt{E_\pi^2 - m_\pi^2 + 4m_N^2}]/2m_N \ , \tag{40}$$

hold simultaneously in a given phase-space point $(\vec{r}, \vec{p})$. Here $\vec{v}_T$ and $v_\parallel$ are, respectively, the transverse and longitudinal components of the pion velocity.

The violation of the last condition implies that the c.m. energy of the NN pair, $\sqrt{s_0}$, is less than the threshold value, necessary for producing a pion with c.m. energy E_π [32]. The relation (40) can be rewritten as

$$t < t_{\rm thr}(E_\pi) \ , \tag{41}$$

where $t_{\rm thr}$ is the solution of the equation $\gamma(t) = \gamma_{\rm thr}$. At high enough E_π or low bombarding energies $E_{\rm lab}$ this equation may have no roots. In this case $\tilde{n}_\pi(t) = 0$ for all t.

The first (second) inequality in Eqs. (38)–(40) is equivalent to the condition that the projectile (target) baryon density is nonzero at the considered space-time point. Let $t_-^p(t_-^t)$ and $t_+^p(t_+^t)$ denote, respectively, the lower and upper time limits when the corresponding inequality holds [if these limits do not exist, $\tilde{n}_\pi = 0$ in a given $(\vec{r}, \vec{p})$ point]. Then we arrive at the following expressions for $t_\pm$:

$$t_+ = \min(t_+^p, t_+^t, t_{\rm thr}) \ , \tag{42}$$

$$t_- = \max(t_-^p, t_-^t) \ . \tag{43}$$

Explicit expressions for $t_\pm$ can be obtained if the function $\xi(t)$ is specified.

Inserting Eqs. (31) and (32) into Eqs. (25) and (27) one obtains the following relation for the pion absorption rate:

$$\tilde{\lambda}_a(t) = \sum_{\alpha=p,t} \lambda_{a\alpha}(t)\Theta(t_+^\alpha - t)\Theta(t - t_-^\alpha) \ , \tag{44}$$

where

$$\lambda_{a\alpha} = \rho_0 \sqrt{\gamma^2(v_\parallel \mp \dot{\xi})^2 + \vec{v}_\perp^{\,2}} \cdot \sigma_{\rm abs}(E'_\alpha) \ , \tag{45}$$

$$E'_\alpha = \gamma E_\pi \cdot (1 \mp \dot{\xi} v_\parallel) \ . \tag{46}$$

Again, the upper and lower signs correspond, respectively, to the projectile and target nucleus. As follows from Eqs. (16), (17), and (44), the pion absorption in the nucleus α ($\alpha = p, t$) is nonzero only if the inequality $t_+^\alpha > t_- + \tau_f$ holds.

All calculations can be done analytically for the free-streaming limiting case, when the mutual deceleration of nuclei is totally disregarded, i.e., for $\dot{\xi}(t) = v_0 = \text{const}$. This approximation was considered earlier in Refs. [12, 13]. The resulting expressions can be obtained by substituting

$$\xi(t) = -R/\gamma_0 + v_0\, t \ , \tag{47}$$

$$\gamma(t) = \gamma_0, \tag{48}$$

into Eqs. (38)–(39). In the most simple case $\vec{p}_{\rm c.m.} = 0$ we get

$$t_\pm^p(\vec{r}_\perp, z) = t_\pm^t(\vec{r}_\perp, -z) = \frac{1}{v_0}\left(\frac{R \pm R_\perp}{\gamma_0} + z\right) \ , \tag{49}$$

where $R_\perp \equiv \sqrt{R^2 - \vec{r}_\perp^{\,2}}$. Assuming that Eq. (40) holds at given E_π and γ_0 (i.e., $t_{\rm thr} = \infty$) and using Eqs. (42)–(43) it is easy to show that in the considered case $t_\pm = t_\pm^p(\vec{r}_\perp, \mp|z|)$. The total pion production time at a given spatial point is equal to

$$t_+ - t_- = \frac{2}{v_0}\left(\frac{R_\perp}{\gamma_0} - |z|\right) \le \frac{2R_\perp}{\gamma_0 v_0} \le \tau_c \ . \tag{50}$$

Here $\tau_c = 2R/\gamma_0 v_0$ is the reaction time in the e.v. frame. From Eqs. (22) and (50) one obtains the necessary condition for the BE effect in the free-streaming approximation [12, 13]

$$\tau_c > \tau_0 \ . \tag{51}$$

As an illustration, Fig. 3 shows the space-time picture of pion production and absorption for pions with $\vec{p}_{\rm c.m.} = 0$ at points along the collision axis ($\vec{r}_\perp = 0$). In the free-streaming approximation the backward (front) boundary of the nucleus α is represented by the straight line $t = t_+^\alpha$ ($t = t_-^\alpha$) on the (t, z) plane. The pion production takes place within the region $(OBCD)$. Pions are hadronized above the dotted lines representing the points $t = t_- + \tau_f$. The shaded region corresponds to the domain $t_- + \tau_f < t < t_+$ where pions are produced in presence of the already formed π mesons. This is the domain where the BE is nonzero. It exists if condition (51) is fulfilled. The vertical dashed line corresponds to world lines of zero-momentum pions produced at fixed z. Within the interval (FG) both the Bose-enhanced pion production and absorption in the projectile and target nuclei take place. Inside the interval (GH) the absorption occurs only in the projectile.

D. Mutual deceleration of the colliding nuclei

Below we describe the parametrization of the function $\xi(t)$ which determines the motion of nuclei in the course of the collision. Instead of using the Woods-Saxon profile for $\dot{\xi}(t)$ [38], we adopt the deceleration law obtained

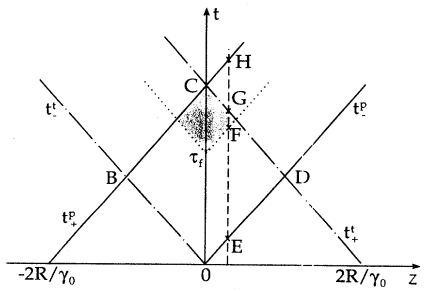

FIG. 3. Space-time picture of a central heavy-ion collision in the free-streaming approximation for the points at the beam axis. Solid (dash-dotted) lines show boundaries of the projectile (target) nucleus. R denotes the radius of the nuclei and γ_0 is their Lorentz factor in the e.v. frame. The shaded region represents the domain where the Bose-stimulated production of pions with zero c.m. momentum takes place.

earlier [23] for ultrarelativistic proton-nucleus collisions.

Let us consider a fast nucleon traversing normal nuclear matter with the instantaneous kinetic energy $E_{\rm rel}$ in the rest frame of the matter. The following equation for the average energy loss per unit path length ($z_{\rm rel}$) of a nucleon was derived in Refs. [23, 24]:

$$\frac{dE_{\rm rel}}{dz_{\rm rel}} = -\frac{E_{\rm rel}}{\lambda_d} , \tag{52}$$

where λ_d is the effective deceleration length. The latter is inversely proportional to the fractional energy loss in a single NN collision. At $E_{\rm rel} \gtrsim 1$ GeV the deceleration length is almost independent of $E_{\rm rel}$ and equals approximately 4 fm [40]. The deceleration law (52) agrees well with the data on average rapidity shifts of leading nucleons observed in pA collisions in a wide range of bombarding energies [24].

In this work we extrapolate Eq. (52) to the case of a nucleus-nucleus collision. Making the transformation from the e.v. frame to the target rest frame and applying Eq. (52) to a projectile nucleon we get the relations $E_{\rm rel} = 2m_N \cdot (\gamma^2 - 1)$, $dz_{\rm rel} = 2\sqrt{\gamma^2 - 1}dt$, where γ is the Lorentz factor of nuclei in the e.v. frame and Eq. (31) was used for the instantaneous nucleon four-velocities. This results in the differential equation

$$\frac{d}{dt}(\gamma^2 - 1)^{-1/2} = \lambda_d^{-1} . \tag{53}$$

Assuming λ_d =const we get the solution for $\gamma(t)$

$$\frac{1}{\sqrt{\gamma^2 - 1}} = \frac{1}{\sqrt{\gamma_0^2 - 1}} + \frac{t}{\lambda_d} . \tag{54}$$

According to this equation the complete mutual stopping of nuclei ($\gamma \to 1$) takes place only asymptotically at $t \to \infty$. From Eq. (54) we obtain the explicit expression for the projectile velocity in the e.v. frame

$$\dot{\xi} = \frac{d\xi}{dt} = \left. \frac{v_0}{\sqrt{1 + \chi^2 + 2\chi \cdot \gamma_0^{-1}}} \right|_{\chi = \frac{v_0 t}{\lambda_d}} . \tag{55}$$

As one can see from this equation, at $t \to \infty$ $\dot{\xi}$ drops rather slowly, as $1/t$. The solution of Eq. (55) can be written analytically

$$\xi(t) = -\frac{R}{\gamma_0} + \lambda_d \ln\left(\chi + \sqrt{1 + \chi^2 + 2\chi \cdot \gamma_0^{-1}}\right) , \tag{56}$$

where the initial condition (33) is used. In the limit $\lambda_d \to \infty$ we arrive at the formulas (47) and (48) of the free-streaming approximation. Relations (54)–(56) were applied for calculating the pion production and absorption rates in accordance with Eqs. (36) and (44).

Of course, initially only the overlapped parts of nuclei are involved in the deceleration process. Therefore, the extension of the energy loss to the entire nuclear volume is a rather crude approximation, especially for the early stage of the reaction. However, we think that the above approach gives a reasonable description of the local energy losses in the overlap region and, therefore, can be applied for calculating the pion production rates even at the initial stage of the reaction.

On the other hand, the compression effects will certainly enhance the friction between the baryonic flows. Besides, a dense cloud of secondary hadrons should lead to an additional stopping of baryons at a later stage of the collision [21]. This may essentially modify the dynamics of nucleon deceleration as compared to the proton-nucleus collision. Bearing this in mind, we consider the deceleration length λ_d as a model parameter which is determined from the fit of observed pion spectra for a given bombarding energy and combination of nuclei. We believe that 4 fm is a reasonable upper limit for λ_d.

Figure 4 represents the space-time region of pion production in 200A GeV central S+S collision. As in Fig. 3, we consider the pions with $\vec{p}_{\rm c.m.} = 0$ produced at different points along the beam axis. Solid and dash-dotted lines correspond, respectively, to the projectile ($t = t_{\pm}^p$) and target ($t = t_{\pm}^t$) boundaries, calculated for λ_d=4 fm by using Eqs. (38) and (39). From Fig. 4, one can see that in the considered case the reaction time, $t_C - t_O$, is about 3 fm/c, which is much larger than the corresponding value $\tau_c \simeq 0.69$ fm in the free-streaming model. Now, the BE effects are possible even at relatively large pion formation times and also for light combinations of nuclei and/or rather high bombarding energies. For example, at $\tau_f = \tau_0 = 2$ fm the BE is predicted inside a shaded region shown in Fig. 4. In contrast, in the free-streaming approximation the BE effects are predicted only for much smaller τ_0 [see Eq. (51)].

The other consequence of the deceleration is a strong time dependence of the pion production rate $\tilde{\lambda}$. The calculation shows that $\tilde{\lambda}$ drops by 2 orders of magnitude when going from the point O to C in Fig. 4. As we shall see later, for the soft pion component this drop can be partly compensated by the BE. Due to the deceleration and absorption effects, the total pion multiplicity is, as a rule, lower than in the free-streaming case.

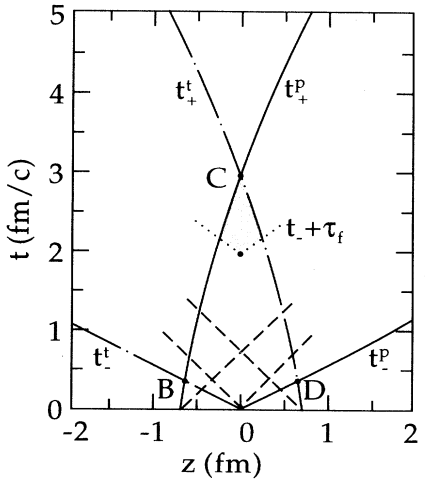

FIG. 4. Dynamical picture of a central 200A GeV S+S collision in the t-z plane ($\vec{r}_\perp = 0$). Solid (dash-dotted) curves represent the projectile (target) boundaries in the case when the deceleration length $\lambda_d = 4$ fm. Dashed lines show the position of the nuclear boundaries in the limit $\lambda_d = \infty$. Other notations are the same as in Fig. 4.

E. Solution of the kinetic equation in limiting cases

In conclusion of this section let us study in more detail some limiting cases when the solution of Eq. (15) may be obtained in an analytic form. For example in the case $\lambda_a = 0, \tau_f = 0$ we have [13]

$$\tilde{n}_\pi = \exp\left[n_\pi^{(0)}\right] - 1 \ , \tag{57}$$

where

$$n_\pi^{(0)} \equiv \int_{-\infty}^{t} d\tau \tilde{\lambda}(\tau) \tag{58}$$

is the pion occupation number in absence of the BE effects. One can see that the pion phase-space density is strongly enhanced if $n_\pi^{(0)} \gtrsim 1$. On the other hand, Eq. (57) overestimates the BE since it does not take into account the finite pion formation time.

The other example which can be studied analytically is the case when the pion production and absorption rates do not depend on t and $\vec{r}$:

$$\tilde{\lambda}, \tilde{\lambda}_a = \text{const.} \tag{59}$$

In particular, such a situation may take place when two half-spaces of nuclear matter interpenetrate without deceleration and one considers the production of pions with $|v_\parallel| < v_0$. Substituting $t_-^\alpha = 0$, $t_+^\alpha = \infty$ into the general formulas (19)–(21), (42), and (43) we get

$$\tilde{n}_\pi(t) = \sum_{k=1}^{\infty} \left(\frac{\tilde{\lambda}}{\tilde{\lambda}_a}\right)^k \left\{1 - e^{-x_k}\left[1 + x_k + \cdots + \frac{x_k^{k-1}}{(k-1)!}\right]\right\} \Theta(x_k) \ , \tag{60}$$

where $x_k \equiv \tilde{\lambda}_a \cdot (t - k\tau_f)$.

The term $k = 1$ in Eq. (60) gives the solution without the BE effects:

$$\tilde{n}_\pi^{(0)} = \frac{\tilde{\lambda}}{\tilde{\lambda}_a}\left[1 - e^{-\tilde{\lambda}_a \cdot (t - \tau_f)}\right] \Theta(t - \tau_f) \ . \tag{61}$$

As we can see from this equation, $\tilde{n}_\pi$ increases linearly with t at small $t - \tau_f$ and reaches the limiting value $\tilde{\lambda}/\tilde{\lambda}_a$ within a time interval $\sim \tilde{\lambda}_a^{-1}$. The terms with $k > 1$ describe the influence of the Bose-stimulated production. At $\tilde{\lambda}_a \tau_f \lesssim 1$ they give rise to "jumps" of $\tilde{n}_\pi$ at $t = 2\tau_f, 3\tau_f, \ldots$.

The asymptotic behavior of $\tilde{n}_\pi$ at large t is essentially determined by the ratio $\tilde{\lambda}/\tilde{\lambda}_a$. In the case of $\tilde{\lambda}_a > \tilde{\lambda}$, as one can see from Eq. (60), the pion occupation number saturates at $t \to \infty$

$$\tilde{n}_\pi \underset{t\to\infty}{\longrightarrow} n_{\rm eq} = \frac{\tilde{\lambda}}{\tilde{\lambda}_a - \tilde{\lambda}} \ . \tag{62}$$

The "equilibrium" value $n_{\rm eq}$ can be obtained assuming that all quantities entering the kinetic equation (15) do not depend on time.

In the opposite case, $\tilde{\lambda}_a < \tilde{\lambda}$, the balance between the absorption and production of pions is not possible and $\tilde{n}_\pi$ grows exponentially at large t. For example, the limit $\tilde{\lambda}_a \tau_f \ll 1$ yields the following relation ($t > \tau_f$):

$$\tilde{n}_\pi = \sum_{k=1}^{[t/\tau_f]} \frac{\tilde{\lambda}^k (t - k\tau_f)^k}{k!} \ . \tag{63}$$

At $\tilde{\lambda}\tau_f \ll 1$ one gets the relation $\tilde{n}_\pi \simeq \exp(\tilde{\lambda} t) - 1$ which may be derived also from Eq. (57).

Of course, the assumption (59) is not realistic. In a real heavy-ion collision $\tilde{\lambda}, \tilde{\lambda}_a$ decrease rapidly at large t due to the deceleration effects. The calculation shows that $\tilde{\lambda}, \tilde{\lambda}_a$ drop more rapidly than t^{-3} at $t \to \infty$. As a consequence, $\tilde{n}_\pi$ saturates at late stages of the reaction. A rough estimate for pion phase-space density may be obtained by substituting Eq. (20) into the r.h.s. of Eq. (15) and comparing the gain and loss terms at $t \sim (k+1)\tau_f$ where $k = 0, 1, \ldots$. We arrive at the following approximate relations for the components of $\tilde{n}_\pi$ defined in Eq. (20):

$$n_0 \sim \tilde{\lambda}(0)/\tilde{\lambda}_a(\tau_f) \ , \tag{64}$$

$$n_{k+1}/n_k \sim \tilde{\lambda}(k\tau_f)/\tilde{\lambda}_a[(k+1)\tau_f] \ . \tag{65}$$

The calculation shows that at the BNL and CERN bombarding energies $n_0 \gg 1$ and $n_{k+1} \lesssim n_k$. A more detailed study of the time dependence of $\tilde{n}_\pi$ will be given in Sec. III C.

III. RESULTS

A. Free-streaming approximation

Let us consider first the limiting case $\lambda_d = \infty, \lambda_a = 0$, disregarding the deceleration and absorption effects. In Refs. [12, 13] we applied this free-streaming approximation to study the production of pions with zero c.m. momentum. Here the results for arbitrary pion momenta are presented. In the considered case the time dependence of the pion production rate is determined by Eq. (36) where λ_0 is time independent. The latter is calculated by substituting (47)–(48) into Eq. (37). A straightforward calculation based on Eqs. (19)–(21) shows that the solution of the kinetic equation for $\tilde{n}_\pi$ is given by Eq. (63) with the replacement $\tilde{\lambda} \to \lambda_0$, $t \to \min(t, t_+ + \tau_f) - t_-$.

The asymptotic value of the pion occupation number may be written as

$$n_{\rm as} \equiv \lim_{t\to\infty} \tilde{n}_\pi = \lambda_0 \, \Delta t \Theta(\Delta t) + \frac{\lambda_0^2}{2!}(\Delta t - \tau_f)\,\Theta(\Delta t - \tau_f) + \frac{\lambda_0^3}{3!}(\Delta t - 2\tau_f)^2\,\Theta(\Delta t - 2\tau_f) + \cdots \ , \tag{66}$$

where $\Delta t \equiv t_+ - t_-$. The terms with $\Delta t > \tau_f$ give the contribution from the BE effect. By substituting (66) into Eq. (23) one can calculate spectra of secondary pions.

The explicit expression for the pion yield may be obtained [12, 13] in the case $p_{\rm c.m.} = 0$. Then Δt is given by Eq. (50) and the volume integration in Eq. (23) results in the following expression for the invariant spectrum of π^- in a central nuclear collision:

$$N(0) \equiv E_\pi \frac{dN_{\pi^-}}{d^3p}\bigg|_{\vec{p}=0} = \frac{m_\pi}{(2\pi\hbar)^3} \cdot \frac{\pi R^3 \beta}{2\gamma_0} \left\{ 1 + \beta \frac{4+\delta}{15}(1-\delta)^4\,\Theta(1-\delta) + \beta^2 \frac{5+2\delta}{90}(1-2\delta)^5\,\Theta(1-2\delta) + \cdots \right\} . \tag{67}$$

Here $\beta \equiv \lambda_0 \tau_c$ and $\delta \equiv \tau_0/\tau_c$ are, respectively, the dimensionless pion production rate and formation time for $p_{\rm c.m.} = 0$ [τ_c is the reaction time defined in Eq. (50)]. The factor outside the curly brackets is the pion yield predicted by the simple convolution model [13]. The expression in the curly brackets gives the correction due to the BE effect. It has a nontrivial A dependence ($\tau_c \propto R \propto A^{1/3}$) and differs from unity for $\delta < 1$ or $\tau_0 < \tau_c$. This condition may be fulfilled only at sufficiently low values of the pion formation time τ_0, heavy combinations of nuclei and/or not too high bombarding energies.

Table I gives characteristic numbers for the case of central Au+Au collisions at bombarding energies 10.7 and 200 GeV/nucleon. The value $\tau_0 = 1$ fm/c is taken in the calculation [41]. The table shows separately the values of nonzero terms on the r.h.s. of Eqs. (66) and (67). The relative contribution of the BE is much smaller in the pion spectra than in the corresponding occupation number, because the spatial domain where the condition (22) holds, occupies only a small fraction of the total volume where pions are produced [12, 13]. Apparently, the very large contribution of the BE for the BNL energy is unrealistic. Indeed, the free-streaming approximation is not justified at this relatively low $E_{\rm lab}$, especially for such a heavy system as Au+Au. The recent experimental data show [42] that a complete baryon stopping takes place in this case.

More detailed information about the pion spectra is given in Figs. 5 and 6 which show the π^- spectra for different values of the rest-frame formation time τ_0. Central Au+Au collisions at 200A GeV are considered in the free-streaming approximation. One can see that the Bose-stimulated production leads to the additional yield of the low-p_T pions (Fig. 5) as compared to the convolution of the $NN \to \pi X$ cross section. The effect is very sensitive to the parameter τ_0. For the reaction considered, the model predicts a nonvanishing BE effect at $\tau_0 < \tau_c = 1.26$ fm/c. According to Fig. 6, the effect may be seen even in the rapidity distribution dN_{π^-}/dy: the model predicts a central rapidity peak if τ_0 is sufficiently small.

Within the free-streaming approximation the width of this peak can be estimated from purely geometrical considerations. Let us consider the production of pions with $p_T = 0$ and nonzero c.m. rapidity y. The straightforward generalization of formulas (49) and (50) for the case $v_{\|\neq 0}$ yields

$$t_+ - t_- \le \frac{2R}{\gamma_0 (v_0 + |v_\|)|} = \frac{2R \cosh y}{\sinh (y_0 + |y|)} , \tag{68}$$

where $y_0 = \operatorname{arctanh}(v_0)$ is the projectile rapidity in the e.v. frame. By using Eqs. (22) and (68) it is easy to see that the BE is significant only in the central rapidity window

$$|y| < \operatorname{arcsinh}\left(\frac{2R}{\tau_0}\right) - y_0 \simeq \ln \frac{2R}{\gamma_0 \tau_0} . \tag{69}$$

Relation (69) generalizes condition (51) for pion rapidities $|y| \neq 0$. It can be fulfilled if $2R > \tau_0 \sinh y_0$. In the case of 200A GeV Au+Au the half-width of the midrapidity peak is equal to 0.92 and 0.23 for $\tau_0 = 0.5$ and 1 fm/c, respectively. One should have in mind that the

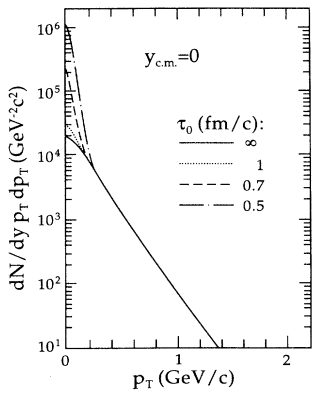

FIG. 5. π^- spectra in 200A GeV central Au+Au collisions versus transverse momentum p_T at longitudinal rapidity $y_{\rm c.m.} = 0$. Shown are the results obtained in the free-streaming approximation for different values of the parameter τ_0.

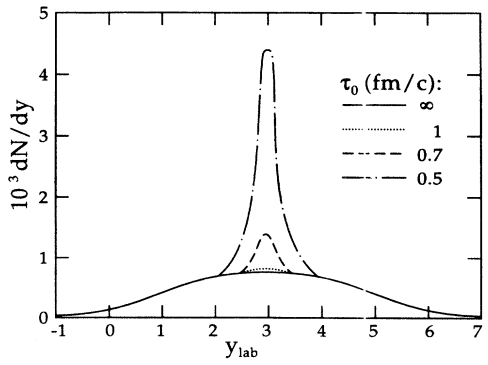

FIG. 6. Same as in Fig. 5 but for pion rapidity distribution.

TABLE I. The characteristics of soft pion production ($p_{\rm c.m.} = 0$) in central Au + Au collisions. Different terms in $n_{\rm as}$ and $N(0)$ give the contributions of corresponding terms of Eqs. (66) and (67).

	$E_{\rm lab} = 10.7A$ GeV	$E_{\rm lab} = 200A$ GeV
τ_c (fm/c)	2.73	1.26
λ_0 (c/fm)	40.7	816
$n_{\rm as}\vert_{\vec{r}=0}$	$2.22\times10^2 + 1.64\times10^4 + 4.62\times10^5$	$1.03\times10^3 + 2.30\times10^4$
$N(0)$ (c^3 GeV^{-2})	$2.74\times10^3 + 7.53\times10^4 + 8.18\times10^5$	$3.17\times10^3 + 1.95\times10^3$

model becomes unrealistic at $\tau_0 \to 0$ when it predicts a very large enhancement of the total pion multiplicity [see Eq. (57)]. In this case one should explicitly take into account the substantial energy losses of baryons due to the pion emission. This, in turn, will suppress the pion production rates and diminish the possible BE effect.

As we shall see later, the qualitative signatures of the BE, predicted in the free-streaming limit, remain also in a more realistic calculation when the deceleration and absorption effects are taken into account. On the other hand, the geometrical conditions for the BE become less restrictive in this case. In particular, effects of Bose-stimulated production may be expected even at relatively large τ_0, high $E_{\rm lab}$ and/or light combinations of nuclei.

B. Comparison with the CERN and BNL experimental data

As was noted earlier, the effects of the projectile-target deceleration change substantially the dynamics of pion production processes and the magnitude of the BE effect. Below we present the results of calculations where the absorption and deceleration processes are taken into account. We consider central collisions of identical nuclei at CERN and BNL bombarding energies: (A) 200A GeV S+S and (B) 10.7A GeV Au+Au. The comparison of observed pion spectra with model predictions can be used to fix the two adjustable parameters introduced in the present approach, namely τ_0 and λ_d.

The analysis shows that the value $\tau_0 \simeq 2$ fm/c gives the best fit of experimental data for both reactions considered. The sensitivity to the choice of τ_0 can be seen in Fig. 7 where the rapidity spectrum of π^- in the reaction (A) is represented for the parameter $\lambda_d = 1.5$ fm/c and various values of τ_0. At $\tau_0 = 2$ fm/c the model agrees fairly well with the experimental data (note that the vertical scale is linear). The pion yield is underestimated at the tails of the rapidity distribution. This may be a consequence of $\pi\pi$ rescatterings disregarded in our model. These final-state interactions will certainly cause some collective expansion of the pion cloud [20] and increase the width of the dN/dy distribution.

Figure 8 presents the results for different choices of the deceleration length λ_d. In this reaction, the best fit is obtained for λ_d=1.5 fm. The comparison with the limiting case $\lambda_d = \infty$ shows that deceleration effects suppress the pion yield by about 50%. The main reason for this suppression is a reduced pion production rate. The direct calculation with $\sigma_{\rm abs} = 0$ shows that the absorption effects are not so important in this case and reduce the pion multiplicity by only about 15%. In the same figure we show the results obtained without the BE effect, i.e., by omitting all terms in Eq. (20) except $k = 0$. It is seen that the BE effects are relatively small in the reaction (A) and can be noticeable only at midrapidity. At $\lambda_d \gtrsim 3$ fm the BE practically vanishes, in agreement with the free-streaming model which does not predict any Bose effect for $\tau_0 = 2$ fm/c and $E_{\rm lab} = 200A$ GeV.

Figure 9 represents the p_T distribution of pions in the same reaction. The "best-fit" parameters $\tau_0 = 2$ fm/c and λ_d=1.5 fm are used in the calculation. One can see that the model underestimates the data at $p_T \gtrsim 1$ GeV/c, which may be also due to neglect of the $\pi\pi$ rescatterings. Only a minor BE effect is predicted at $p_T \lesssim 0.1$ GeV/c

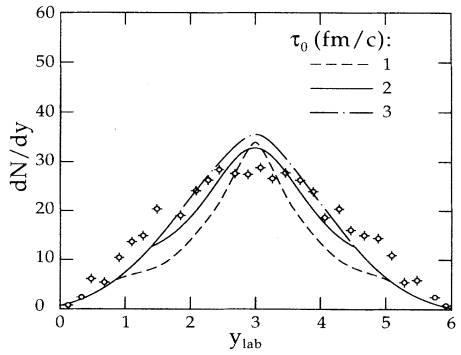

FIG. 7. π^- rapidity spectra in 200A GeV central S+S collisions calculated for $\lambda_d = 1.5$ fm and different values of τ_0. Experimental data (open dots) correspond to the rapidity distribution of negative hadrons [1, 43].

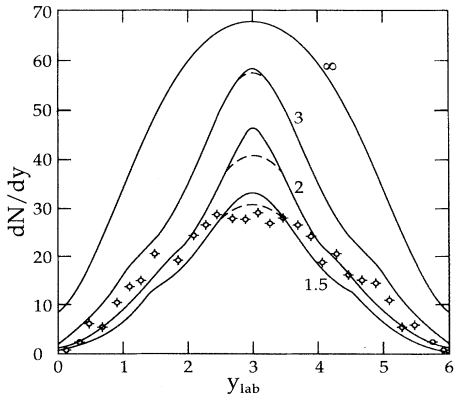

FIG. 8. Same as in Fig. 7, but for $\tau_0 = 2$ fm/c and different λ_d (shown in fm at the corresponding curves). Solid (dashed) lines represent the results with (without) the inclusion of the BE effects.

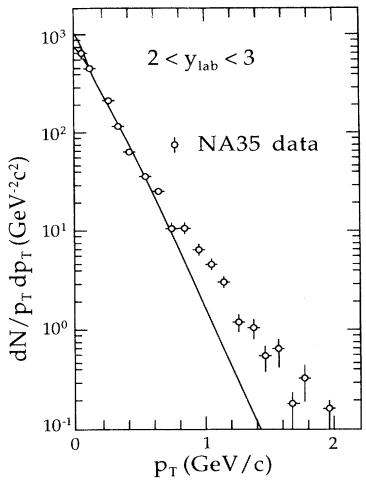

FIG. 9. p_T distributions of π^- mesons in 200A GeV central S+S collisions calculated for $\lambda_d = 1.5$ fm and $\tau_0 = 2$ fm/c. The notations are the same as in Figs. 7 and 8.

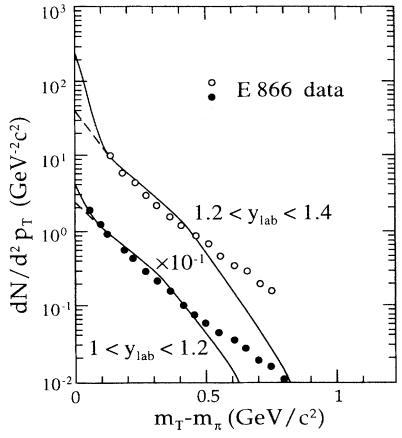

FIG. 11. Same as in Fig. 10, but for the pion p_T spectra in two regions of pion rapidity. $m_T \equiv \sqrt{m_\pi^2 + p_T^2}$ is the transverse pion mass. The parameter $\kappa = 3$.

(cf. Fig. 5). As will be seen in the next section, the BE gives a small contribution in the considered cases since the most interesting kinematic domain $p_T \simeq 0$, $y_{\text{c.m.}} \simeq 0$ has a relatively small weight in the integrated (rapidity or p_T) distributions.

The results for the reaction (B) are shown in Figs. 10 and 11. Again, the data are reproduced fairly well with the choice τ_0=2 fm/c. However, a higher deceleration length, λ_d =4 fm, which coincides with the estimate given in Sec. II D, is preferable in this case. The other qualitative difference with the case (A) is the role of pion absorption. As one can expect from Fig. 1, the absorption effects are much more important at the BNL bombarding energy. The calculation shows that the model overestimates the pion yield in this reaction unless an additional absorption is introduced.

The additional absorption can be explained by the compression of baryon flows [39]. Within the multifluid approach the compression ratios $\rho/\rho_0 \sim 2 - 3$ are predicted [21, 24] for this reaction. On the other hand, no significant compression has been obtained for reaction (A). To take into account the additional absorption at the BNL energy we introduced the compression factor $\kappa = \rho_\alpha/\rho_0$ in the r.h.s. of Eq. (27), replacing ρ_α^2/ρ_0 by $\rho_\alpha\kappa$. One power of κ is effectively cancelled out by integrating over the Lorentz-contracted nuclear volume [see Eq. (17)]. The absorption rate now becomes $\kappa\tilde{\lambda}_a$ where $\tilde{\lambda}_a$ is given by Eqs. (44) and (45).

According to Figs. 10 and 11, a reasonable agreement with the data may be achieved by choosing the parameter $\kappa \simeq 3$. It is seen that the BE at low p_T and midrapidity is more noticeable than in the reaction (A). More definite conclusions may be drawn if it would be possible to extend measurements to the region $p_T < 0.1$ GeV/c.

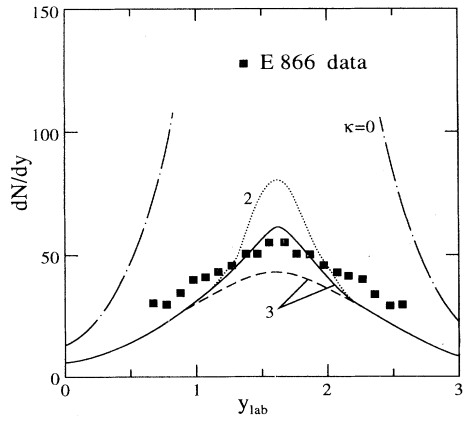

FIG. 10. π^+ rapidity spectra in 10.7A GeV central Au+Au collisions calculated for $\lambda_d = 4$ fm, $\tau_0 = 2$ fm/c and different values of the compression parameter κ. The dashed line shows the result without BE (for $\kappa = 3$). Experimental data are taken from Ref. [42].

C. Possible signatures of the Bose-enhancement effect

As discussed in the previous section, single differential spectra like dN/dy or dN/dp_T show a rather low sensitivity to the BE effect, especially for those values of model parameters which are favored by experimental data. Therefore, it is desirable to find observables which are more sensitive to this effect. The double-differential pion spectra at low p_T and small c.m. rapidities are rather promising. Of course such measurements demand much better statistics than it is available now. As shown in Fig. 12, even in the case of a light combination like S+S at 200A GeV, one may expect a rapid change of double differential spectra at $p_T \to 0$ due to the BE effect [44]. One can see that at $p_T = 0.1$ GeV/c this effect gives only a minor ($\sim 10\%$) contribution in the central rapidity region. On the other hand, its contribution grows to the level of $\sim 100\%$ if $p_T \to 0$. It is worth noting

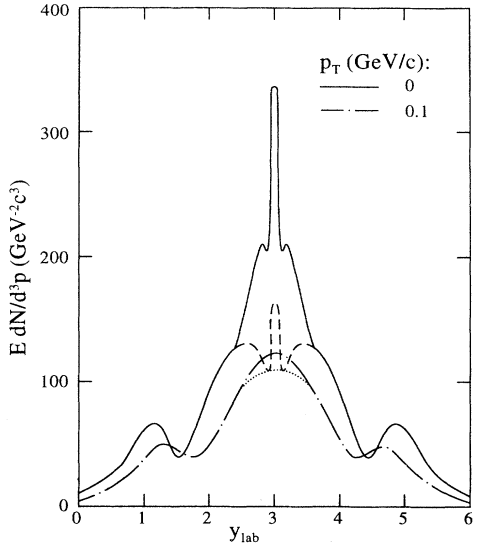

FIG. 12. Double-differential spectra of π^- in 200A GeV central S+S collisions vs pion rapidity at fixed values of p_T. The choice of model parameters is the same as in Fig. 9. Solid and dash-dotted lines show the results for $p_T = 0$ and 0.1 GeV/c, respectively. The dashed and dotted lines represent the corresponding calculation without the BE effects.

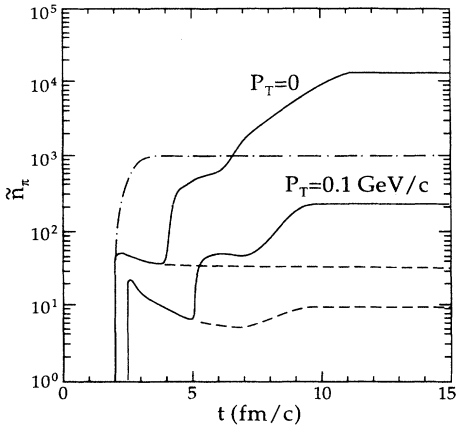

FIG. 13. Time dependence of $\tilde{n}_\pi$ in the point $\vec{r} = 0$ for pions with $y_{c.m.} = 0$ produced in 200A GeV central Au+Au collisions. The solid lines show the results of calculation with the parameters $\tau_0 = 2$ fm/c, $\lambda_d = 4$ fm, $\kappa = 1$. The dashed lines are calculated without BE. The dash-dotted line represents the results for $p_T = 0$ in the free-streaming limit ($\lambda_d = \infty, \kappa = 0$).

that the pion spectra in Fig. 11 correspond to the "almost" double-differential distributions since the rapidity windows are rather narrow. The region $1.2 < y_{lab} < 1.4$ is near midrapidity ($y_{lab} \simeq 1.6$) and it is not surprising that at $p_T \to 0$ the model predicts rather large BE factor (~ 5) in this case.

The rapid variation of the pion yield with the transverse momentum may be explained as follows. With increasing pion transverse velocity, the time available for the pion production, $t_+ - t_-$, decreases while the pion formation time, Eq. (5), increases. As a consequence, the region where condition (22) is satisfied becomes smaller, if it exists at all. More information is given in Fig. 13 where the pion occupation numbers for $p_T = 0$ and 0.1 GeV/c are compared for the 200A GeV Au+Au collision. One can see that the BE factor for asymptotic values of $\tilde{n}_\pi$ drops by more than 1 order of magnitude when going from zero transverse momentum to $p_T = 0.1$ GeV/c.

Due to the BE, the time interval where $\dot{\tilde{n}}_\pi$ is essentially nonzero, δt, increases by an order of magnitude, from $\delta t \sim 1$ to 5–10 fm/c, for $p_T \lesssim 0.1$ GeV/c. Such a qualitative difference in the dynamics of pion production should be reflected in the $\pi\pi$-correlation function $C(\vec{p}_1, \vec{p}_2)$. It is defined as the normalized probability to detect simultaneously two pions with momenta $\vec{p}_1, \vec{p}_2$. At small relative momenta $C > 1$ due to the symmetrization of the two-pion wave function [45]. The characteristic sizes and "lifetimes" of pion emitting source were extracted from the $\pi\pi$ interferometric measurements [46].

Leaving the detailed study of $\pi\pi$-correlations for the future, here we restrict ourselves to a short remark. Assuming a purely incoherent pion emission, one can express [45] the function C via the four-dimensional Fourier transforms of the pion occupation numbers $\tilde{n}_\pi(t, \vec{r}, \vec{p}_{1,2})$ with the corresponding wave vector $q^i = (p_1^i - p_2^i)/\hbar$ where $p_{1,2}^i$ are the pion four-momenta. The increase of the pion source lifetime δt due to the Bose-stimulated pion emission should give rise to a narrow peak in $C(\vec{p}_1, \vec{p}_2)$ at small $|E_1 - E_2| \sim \hbar/\delta t \lesssim 50$ MeV. This peak should be more pronounced for the pion pairs with $p_T^{(1,2)} \lesssim 0.1$ GeV/c, $|y_{c.m.}^{(1,2)}| \lesssim 0.5$. Heavy combinations of nuclei are preferable for this analysis. Unfortunately, up to now no measurements at sufficiently low p_T have been carried out. Nevertheless, we encourage experimentalists to perform such measurements with Au beams at BNL and Pb beams at CERN.

As follows from the above calculations a rather sharp peak of the pion phase-space distribution is predicted around the central point $\vec{r} = 0$, $\vec{p} = 0$ at the initial stage of the reaction. One should bear in mind that this result is obtained within the quasiclassical approximation. Due to the uncertainty principle the particle distributions must be smoothed out over the phase-space cells of the volume $(2\pi\hbar)^3$ [13]. Therefore, in a more refined quantum mechanical approach the maximal pion occupation numbers will be lower. However, we do not expect a significant change of pion spectra, predicted by the present model, because these spectra are obtained by averaging over a large spatial volume of the pion emitting source.

IV. SUMMARY

The main results of the present paper can be summarized as follows.

(1) Experimental data for nuclear collisions at CERN energies imply large phase-space occupation numbers of

pions with $y_{\mathrm{c.m.}} \simeq 0$, $p_T \simeq 0$.

(2) The present model can easily explain the enhanced low-p_T yield of pions observed at CERN and BNL energies as a manifestation of the Bose-stimulated pion production. However, existing data neither confirm nor exclude this explanation. Measurements of extra-soft ($p_T <$ 50 MeV/c) pion yields will be decisive for this mechanism.

(3) The Bose-enhancement effect should be more prominent in double-differential pion spectra and may produce a central rapidity peak for pions with $p_T \lesssim 0.1$ GeV/c. High statistics measurements in this kinematic region are crucial to pin down this effect.

(4) The Bose-stimulated pion production should induce a narrow peak in the $\pi\pi$-correlation function at small difference of pion c.m. energies, $|E_1 - E_2| \lesssim 50$ MeV. The corresponding measurements should be performed for samples of pions with small p_T and $|y_{\mathrm{c.m.}}|$.

To make the model more realistic, it will be necessary to develop a more consistent treatment of the dynamics of baryon flows, e.g., by using the multifluid or kinetic approach. Then the energy transfer from baryons to the mesonic subsystem can be included explicitly. In particular, it would be interesting to investigate the influence of the BE on the stopping of baryons. A more rigorous study of pion absorption processes requires the explicit inclusion of baryon and meson resonances. Final state interactions and the $\pi\pi$ rescattering in a dense meson cloud must also be investigated. A smooth distribution in pion formation times should be introduced instead of the step function used above. We hope to apply the model for studying the possibility of Bose condensation of pions and the evolution of chiral symmetric states in high-energy heavy-ion collisions.

ACKNOWLEDGMENTS

The authors thank G. A. Leksin, U. Katscher, A. E. Kudryavtsev, and Yu. E. Pokrovsky for valuable discussions. Two of us (I.N.M. and L.M.S.) appreciate the warm hospitality and support provided to them by the Institute für Theoretische Physik der J. W. Goethe Universität, Frankfurt am Main. This work was supported in part by the EU-INTAS Grant No. 94-3405, the International Science Foundation (Soros) Grant No. N8Z000, and by the Deutsche Forschungsgemeinschaft.

[1] H. Ströbele *et al.*, NA35 Collaboration, Z. Phys. C **38**, 89 (1988).
[2] T. Akesson *et al.*, HELIOS Collaboration, Z. Phys. C **46**, 361 (1990).
[3] A. Breakstone *et al.*, Phys. Lett. B **132**, 463 (1983).
[4] W. Bell *et al.*, Z. Phys. C **27**, 191 (1985).
[5] E. Shuryak, Phys. Lett. B **207**, 345 (1988); M. Kataja, and P.V. Ruuskanen, *ibid.* **243**, 181 (1990); U. Ornik and R.M. Weiner, *ibid.* **263**, 503 (1991).
[6] J. Sollfrank, P. Koch, and U. Heinz, Z. Phys. C **52**, 593 (1991); H.W. Barz, G.F. Bertsch, D. Kusnezov, and H. Schulz, Phys. Lett. B **254**, 332 (1991).
[7] H. Sorge, Phys. Rev. C **49**, R1253 (1994).
[8] S. Gavin and P.V. Ruuskanen, Phys. Lett. B **262**, 326 (1991).
[9] G.M. Welke and G.F. Bertsch, Phys. Rev. C **45**, 1403 (1992).
[10] H.W. Barz, G.F. Bertsch, P. Danielewicz, and H. Schulz, Phys. Lett. B **275**, 19 (1992); H.W. Barz, P. Danielewicz, H. Schulz, and G.M. Welke, *ibid.* **287**, 40 (1992).
[11] V. Koch and G.F. Bertsch, Nucl. Phys. **A552**, 591 (1993).
[12] I.N. Mishustin, L.M. Satarov, J. Maruhn, H. Stöcker, and W. Greiner, Phys. Lett. B **276**, 403 (1992).
[13] I.N. Mishustin, L.M. Satarov, J. Maruhn, H. Stöcker, and W. Greiner, Z. Phys. A **342**, 309 (1992).
[14] In the case of the 200A GeV S+Pb collision an order of magnitude smaller n_π was extracted from the $\pi\pi$-correlation data by G.F. Bertsch, Phys. Rev. Lett. **72**, 2349 (1994). But this estimate was obtained for n_π averaged over all p_T. By using the exponential p_T distribution assumed in that work, it is easy to show that the corresponding pion occupation number at $p_T = 0$ should be higher by a factor of 4.
[15] A.A. Anselm and M.G. Ryskin, Phys. Lett. B **266**, 482 (1991).
[16] In the present work as well as in [12,13] we assume a hadronic scenario of a nuclear collision. However, our approach can be reformulated also in terms of the quark-gluon or parton degrees of freedom. For example, instead of an inelastic NN collision one can consider the excitation and breakup of a quark-gluon string. The Bose-statistical effects in the fragmentation of an isolated string have been already studied by M.G. Bowler, Z. Phys. **29**, 617 (1985). In the case of a nuclear collision the Bose-statistical effects may severely modify the probability of string fragmentation as compared to the vacuum case.
[17] R. Anishetty, P. Koehler, and L. McLerran, Phys. Rev. D **22**, 2793 (1980).
[18] N.N. Nikolaev, Usp. Fiz. Nauk **134**, 369 (1981) [Sov. J. Usp. **24**, 531 (1981)].
[19] The Bose-enhancement effects are strongly suppressed [13] by the finite pion formation time. Huge "laserlike" effects in pion production predicted by S. Pratt, Phys. Lett. B **301**, 159 (1993), are apparently overestimated because of the assumption of a simultaneous pion emission.
[20] U. Katscher, D.H. Rischke, J.A. Maruhn, W. Greiner, I.N. Mishustin, and L.M. Satarov, Z. Phys. A **346**, 209 (1993).
[21] U. Katscher, Doctor thesis, University of Frankfurt/M, 1994; U. Katscher *et al.* (unpublished).
[22] Yu.B. Ivanov, Nucl. Phys. **A474**, 669 (1987).
[23] L.M. Satarov, Sov. J. Nucl. Phys. **52**, 264 (1990).
[24] I.N. Mishustin, V.N. Russkikh, and L.M. Satarov, Sov. J. Nucl. Phys. **54**, 429 (1991).
[25] H. Bebie, P. Gerber, J.L. Goity, and H. Leutwyler, Nucl. Phys. **B378**, 95 (1992).
[26] Here we do not include explicitly πN rescatterings. The

πN interactions are taken into account in Eq. (2) only via the pion absorption in πNN collisions (see Sec. II B). At high energies the phase-space density of nucleons is relatively small in the central rapidity region, populated mostly by pions. For this reason the elastic πN rescatterings are not so important for pions at midrapidity. As shown in Ref. [21], this is not the case for the proton rapidity spectra which are rather sensitive to these rescatterings.

[27] The accuracy of such a procedure has been discussed in Ref. [13].

[28] N.S. Amelin, K.K. Gudima, and V.D. Toneev, Sov. J. Nucl. Phys. **51**, 1093 (1990).

[29] As known from experimental data on pp collisions [see V.G. Grishin, *Inclusive Processes in Hadron Interactions at High Energies* (Energoizdat, Moscow, 1982)] a considerable fraction of pions is produced indirectly, i.e., through the decay of resonances. The main contribution at midrapidity is given by the formation and decay of the relatively short-lived $\rho(770)$ resonances. For purely kinematic reasons the fraction of direct pions is larger in the low-p_T region and the role of long-lived $\omega(783)$ resonances may be more important in this case. As noted by S.S. Padula and M. Guylassy, Nucl. Phys. **A544**, 537c (1992), the LUND string model, used by many authors, underestimates the fraction of direct pions, by a factor of 2. In this work we consider τ_0 as the model parameter, bearing in mind that the indirect pion production may increase the effective formation time as compared to the value predicted by the uncertainty principle.

[30] J.D. Bjorken, Phys. Rev. D **27**, 140 (1983).

[31] Due to the mutual deceleration of interacting baryonic flows, the relative velocities of nucleons from different flows may become comparable to those for NN pairs inside each flow. In this case the inter- and intraflow terms of the pion source should both be considered. However, we do not expect the qualitative change of the results since both contributions become relatively small in the vicinity of the pion production threshold.

[32] Normally t_+ and t_- coincide with the initial and final times of the projectile-target overlap. However, during the mutual deceleration of interacting nuclei $\tilde{\lambda} \propto \sigma_{\rm inv}(\sqrt{s_0}, \vec{p})$ may vanish even at the stage of geometrical overlap when the c.m. energy per nucleon, $\sqrt{s_0}$, becomes less than the threshold energy for producing a pion with given momentum $\vec{p}$ in a single NN collision (see Sec. II C). In this case t_+ corresponds to the instant of time when the threshold is reached.

[33] T. Ericson and W. Weise, *Pions and Nuclei* (Clarendon Press, Oxford, 1988).

[34] A. Engel, W. Cassing, U. Mosel, M. Schäfer, and Gy. Wolf, Nucl. Phys. **A572**, 657 (1994).

[35] J. Hüfner, Phys. Rep. C **21**, 1 (1975).

[36] B.G. Ritchie, Phys. Rev. C **28**, 926 (1983).

[37] P. Danielewicz and G.F. Bertsch, Nucl. Phys. **A533**, 712 (1991).

[38] D. Vasak, H. Stöcker, B. Müller, and W. Greiner, Phys. Lett. **93B**, 243 (1980).

[39] To avoid misunderstanding, we would like to note that the model takes into account the "kinematic" compression determined by the gamma factor of the baryon flow. In the region where both nuclei overlap geometrically, the total baryon density in the equal velocity frame equals $2\rho_0\gamma$.

[40] At high energies, $\lambda_d \simeq (\rho_0 \sigma_{NN}^{\rm in} k_E)^{-1}$ where $k_E \simeq 0.5$ is the inelasticity coefficient in a single NN collision [24].

[41] The minimal number of nucleons, for which the condition (51) still holds at $\tau_0 = 1$ fm/c and $E_{\rm lab} = 200A$ GeV, is 156. A similar estimate in the case of lighter combination, S+S, shows that the BE may be expected only for $E_{\rm lab} < 95\,(24)A$ GeV if $\tau_0 = 1\,(2)$ fm/c.

[42] M. Gonin *et al.*, Nucl. Phys. **A553**, 799c (1993).

[43] J. Bächler *et al.*, NA35 Collaboration, Phys. Rev. Lett. **72**, 1419 (1994).

[44] The side minima of the pion spectrum at $p_T = 0$ in the central rapidity region appear due to specific energy dependence of the quasideuteron component of pion absorption which becomes large at low pion velocities in the rest frame of the baryonic flow (see Sec. II B).

[45] D.H. Boal, Rev. Mod. Phys. **62**, 553 (1990).

[46] A. Bamberger *et al.*, Phys. Lett. B **203**, 320 (1989); J. Baechler *et al.*, Nucl. Phys. **A525**, 327c (1991); T. Abbot *et al.*, *ibid.* **A525**, 531c (1991).

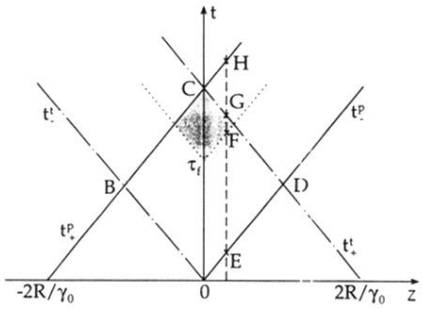

FIG. 3. Space-time picture of a central heavy-ion collision in the free-streaming approximation for the points at the beam axis. Solid (dash-dotted) lines show boundaries of the projectile (target) nucleus. R denotes the radius of the nuclei and γ_0 is their Lorentz factor in the e.v. frame. The shaded region represents the domain where the Bose-stimulated production of pions with zero c.m. momentum takes place.